

Supporting Information

Effective surface diffusion of nickel on single crystal β -Ga₂O₃ for Schottky barrier modulation and high thermal stability

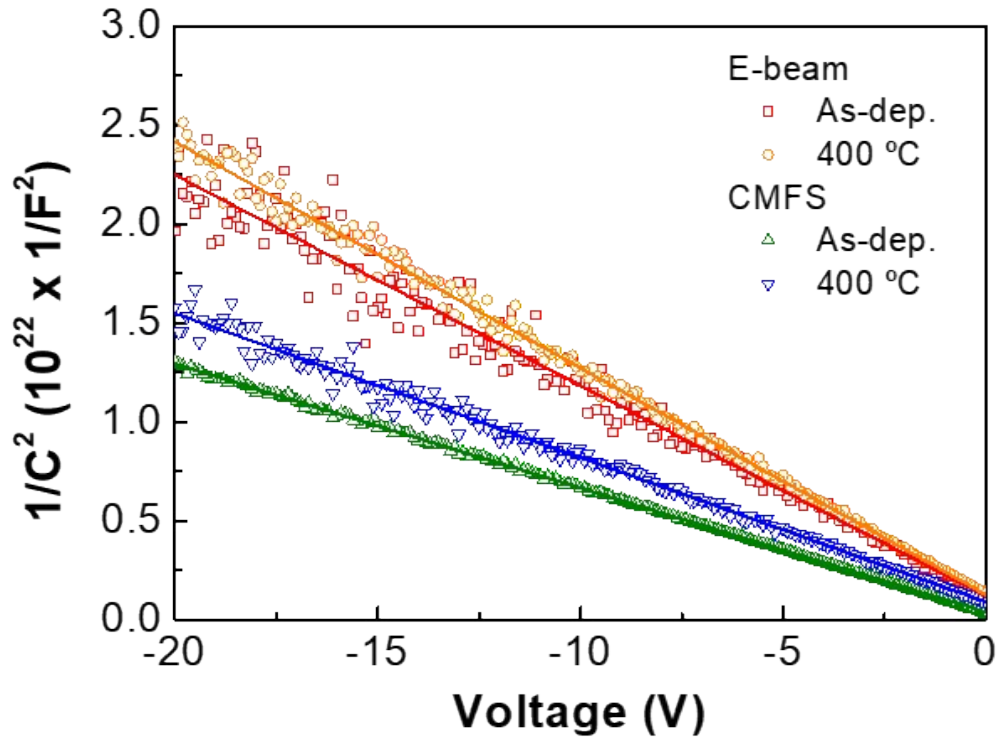
Hojoong Kim,^a Sinsu Kyoung,^b Taiyoung Kang,^b Jang-Yeon Kwon,^c Kyung Hwan Kim,^d and
You Seung Rim^{*,a}

^aSchool of Intelligent Mechatronics Engineering, Sejong University, 209 Neungdong-ro,
Gwangjin-gu, Seoul 05006, Republic of Korea. E-mail: youseung@sejong.ac.kr

^bResearch and Development, Powercubesemi Inc., Sujeong-gu, Seongnam-si, Gyeonggi-do
13449, Republic of Korea

^cSchool of Integrated Technology and Yonsei Institute of Convergence Technology, Yonsei
University, Yeonsu-gu, Incheon 21983, Republic of Korea

^dDepartment of Electrical Engineering, Gachon University, Sujeong-gu, Seongnam-si,
Gyeonggi-do 13120, Republic of Korea



| Deposition methods | Doping concentration (N_d-N_a , cm^{-3}) | |
|--------------------|---|-----------------------|
| | As-dep. | 400 °C |
| E-beam | 2.66×10^{16} | 2.47×10^{16} |
| CMFS | 4.52×10^{16} | 3.88×10^{16} |

Fig. S1. Capacitance-voltage (C - V) measurement on the CMFS deposited and E-beam evaporated Ni/ β -Ga₂O₃ SBDs with post-annealing. The doping concentration (N_d-N_a) of drift layer was calculated about $3 \times 10^{16} \text{ cm}^{-3}$ shown in the table.

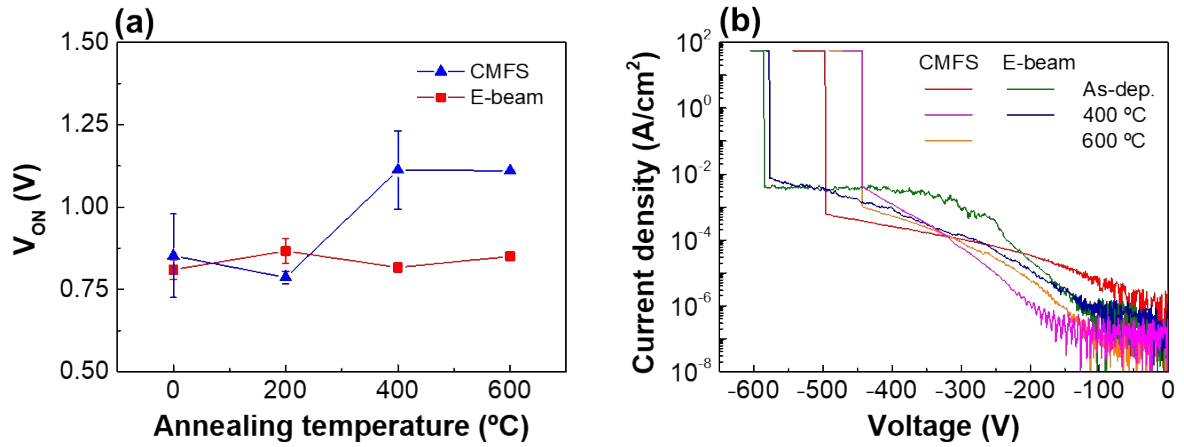
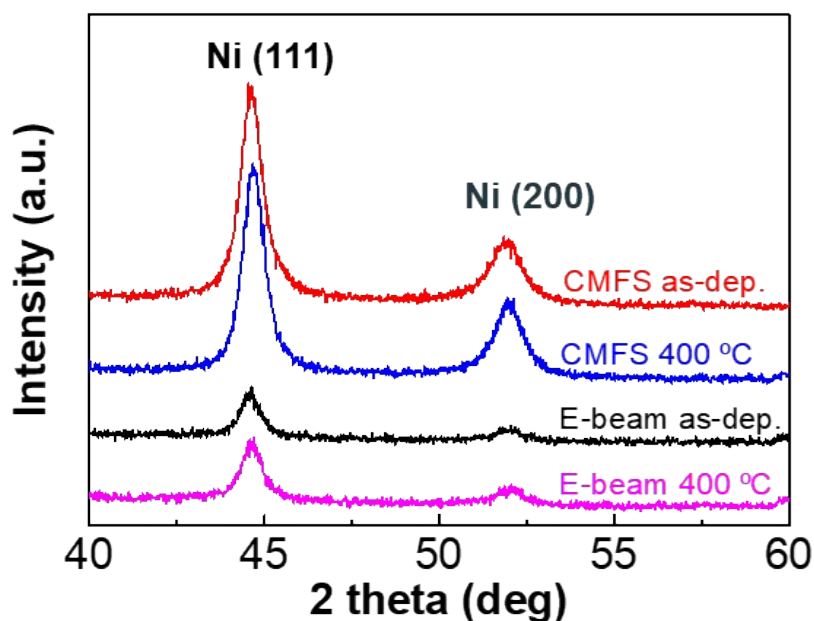


Fig. S2. (a) The variations of the onset voltage (V_{ON}) and (b) reverse breakdown voltage (V_{BR}) on CMFS deposited and E-beam evaporated Ni/ β -Ga₂O₃ SBDs. The V_{BR} of CMFS-Ni SBDs was varied -443 to -496 V, while which of E-beam evaporated Ni-based SBDs was varied -577 to -585 V with post-annealing temperature. In general, the reverse leakage current in the SBDs is related to the SBH, because the thermionic emission current across the SBH is a dominant component of the leakage current. In addition, some phenomena, such as field-emission, image force lowering effect, and barrier inhomogeneity can lower the SBH value. The 400 $^{\circ}C$ annealed CMFS-Ni devices have relatively higher and homogeneous SBH rather than the E-beam devices, which can lead to the low leakage current. However, it seems that there are some carrier trap regions in CMFS-Ni/ β -Ga₂O₃ interface, which can be accelerated to the impact ionization, lowering the V_{BR} value.



| Ni (111) | 2θ (deg) | FWHM (deg) | Lattice constant (nm) | Average grain size (nm) |
|----------------|----------|------------|-----------------------|-------------------------|
| CMFS as-dep. | 44.65 | 0.73 | 0.410 | 11.51 |
| CMFS 400 °C | 44.69 | 0.73 | 0.388 | 11.59 |
| E-beam as-dep. | 44.60 | 0.64 | 0.439 | 13.03 |
| E-beam 400 °C | 44.63 | 0.69 | 0.423 | 12.14 |

Fig. S3. The XRD analysis of the Ni with CMFS and E-beam evaporation methods. The diffraction peaks at $2\theta = 44.6^\circ$ and 51.9° were assigned to the (111) and (200) crystal planes of the Ni. (JCPDS #04-0850) The table shows the parameters of Ni (111) peaks, which are the 2θ center of peak, full width at half maximum (FWHM), lattice constant, and average grain size calculated using the Scherrer equation. All Ni peaks were slightly shifted to the increasing 2θ angle after post-annealing due to the decrease in the lattice constant with relaxation of crystal.

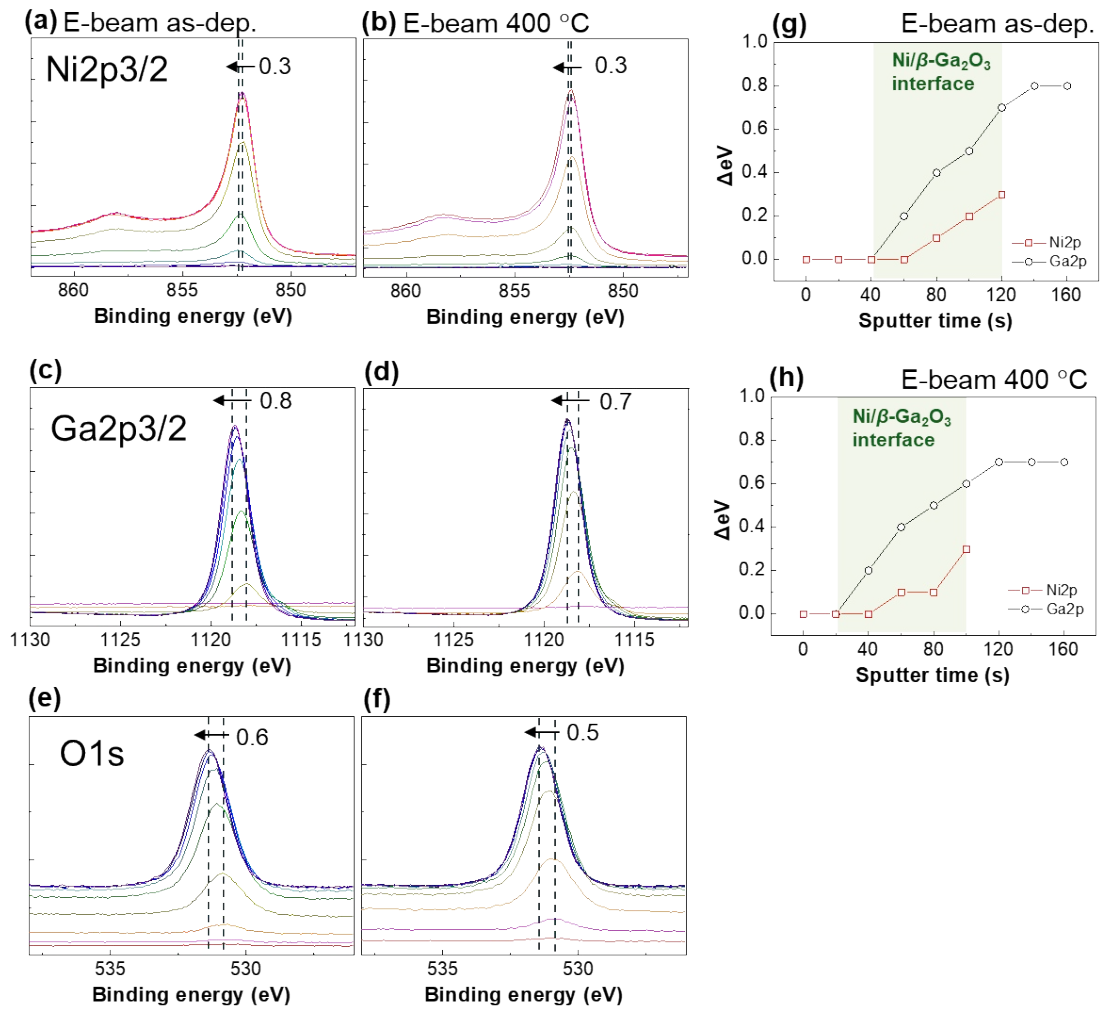


Fig. S4. The XPS depth-profiling analysis with the E-beam evaporated Ni/ β -Ga₂O₃ interface. (a,c,e) As-deposited and (b,d,f) post-annealed at 400 °C with Ni_{2p}, Ga_{2p}, and O_{1s} spectrums, respectively. (g, h) The shift of binding energies of Ni_{2p} and Ga_{2p} peaks as increasing interfacial depth. No additional Ni diffusion was identified with post-treatment.